Proceedings of the 3rd International Conference on the Frontiers of Plasma Physics and Technology (PC/5099)

Laser-Induced Breakdown Spectroscopy for Microanalysis

Y. Godwal, M.T. Taschuk, S.L. Lui, Y.Y. Tsui and R. Fedosejevs

Department of Electrical and Computer Engineering, University of Alberta, Edmonton, AB, Canada T6G 2V4

Abstract Laser induced breakdown spectroscopy is a fast non-contact technique for the analysis of the elemental composition of any sample. Our focus is to advance this technique into a new regime where we use pulse energies below 100 μJ. This regime is referred to as microLIBS or μLIBS. Preliminary pulse emission scaling of Na in latent fingerprints has been investigated for $\sim$ 130 fs, 266 nm pulses with energies below 15 μJ. The single shot limit of detection is expected to be approximately 3.5 μJ for this case. A 2D map of a fingerprint on a Si wafer has been successfully acquired using 5 μJ pulses. The detection sensitivity of micro-laser-induced breakdown spectroscopy (μLIBS) is improved by coupling it with a resonant dual-pulse method called laser ablation-laser induced fluorescence (LA-LIF). This technique was investigated using a waterjet sample containing a low concentration of Pb by weight as an analyte which was ablated by a 266 nm, frequency-quadrupled Q-switched Nd:YAG laser at an energy of $\sim$ 170 μJ. After a short delay the resulting plume was re-excited with a nanosecond laser pulse tuned to a specific transition for the element of interest. In the case of the resonant dual-pulse LIBS the limit of detection was found to be 73 ppb for Pb in water. This result is promising and could be implemented with fiber or microchip lasers with multi-kHz repetition rates as excitation sources for a portable μLIBS water monitoring system or a fingerprint scanner.

1 Introduction

Laser-induced breakdown spectroscopy (LIBS) is an elemental characterisation technique that examines the spectrally resolved emission from a laser-induced plasma to determine the elemental composition of a sample. A short intense laser pulse is used to ionize a small area of a sample. The sample may be in the gas, liquid or solid phase. The hot dense plasma created by the laser pulse expands into the ambient gas and cools rapidly during the initial expansion. As the plasma cools, electrons and ions recombine, emitting electromagnetic radiation at wavelengths characteristic of the elemental composition of the original target. The key advantages of LIBS are:

1. Measurement speed: A LIBS measurement can be performed in well under a millisecond
2. Universal sensitivity: LIBS can detect all conventional elements in solid, liquid or gaseous form
3. Limited sample preparation: little or no sample preparation is required.
4. Environmentally robust: LIBS can be performed under an extremely broad range of conditions

5. Portable: LIBS systems can be made portable based on small compact laser sources and detectors with a little effort, especially compared to alternative techniques

For a summary of current state of the art for the LIBS technique, the reader is referred to either of two recent books devoted to LIBS [1, 2]. The potential of LIBS for use in hostile environments such as in nuclear or fusion reactor settings or for study of radioactive materials has been demonstrated by a number of groups [3–7]. The application of LIBS to radioactive elements has been studied by Wachter et al. [3] and Stoffels et al. [5]. Remote inspection of nuclear power reactor fittings has been demonstrated by Davies et al [4] and Whitehouse et al. [7]. Study of dust on interior tokamak surfaces has been performed by [8].

One of the key disadvantages of the LIBS technique until recently has been the large laser energies required. In order to improve the sensitivity the LIBS technique has typically employed laser pulse energies in the range of 10-100 mJ, focal spot sizes on the order of 100 μm, and an accumulation of 10-100 spectra for a single measurement. In some applications, a second laser pulse is used to reheat the ablation plume, or to selectively excite a specific analyte. This approach is known as dual-pulse LIBS, and has recently been reviewed [9].

This article reports on the expansion of the realm of high sensitivity LIBS to much lower pulse energies. This new regime, referred to as microLIBS or μLIBS, utilizes pulse energies below 100 μJ. This extension to the LIBS technique allows the probing of smaller sample spots for microanalysis applications, and would allow the use of fiber or microchip lasers which currently produce pulse energies in the range of 1 to several hundreds of microjoules. This technique will allow online monitoring of effluent pollution in industrial settings and may, with further development, be applied to online, real time verification of drinking water standards.

Our group has studied μLIBS for microanalysis [10–13]. Rieger et al. studied the scaling of LOD with energy, demonstrating LODs comparable to high energy LIBS experiments [10]. Cravetchi et al. demonstrated single-shot classification of aluminum alloy precipitates [11], followed by the acquisition of a 2D surface map of an aluminum alloy sample [12]. Taschuk et al. recently demonstrated μLIBS detection and mapping of latent fingerprints using $\sim$ 130 fs, $\sim$ 85 μJ pulses at 400 nm [13].

In this paper, two recent applications of μLIBS will be presented and potential scaling to microfluidic lab on a chip applications will be proposed. The first is an extension of the mapping of latent fingerprints to pulse energies compatible with fiber or microchip lasers. The second is the detection of Pb in water using a dual-pulse μLIBS technique. In our case, the second pulse is tuned to a resonant absorption for Pb, selectively enhancing the Pb emission and thus improving the achievable LOD. This technique will be of significant interest in online monitoring of industrial effluents and may, with further developement, be applicable to online, near real-time verification of drinking water standards.

Optical detection techniques for latent fingerprints have been studied by many groups [14–18]. Laser-induced fluoresence for fingeprint detection was first demonstrated in 1976 by Dalyrymple et al. [14]. Remote LIBS detection of latent fingerprints was recently demonstrated by Lopez-Moreno et al. [19]. A more detailed discussion of the fingerprint literature is given in [13]. In the present paper, the scaling of μLIBS fingerprint detection and mapping to much lower energies is investigated.

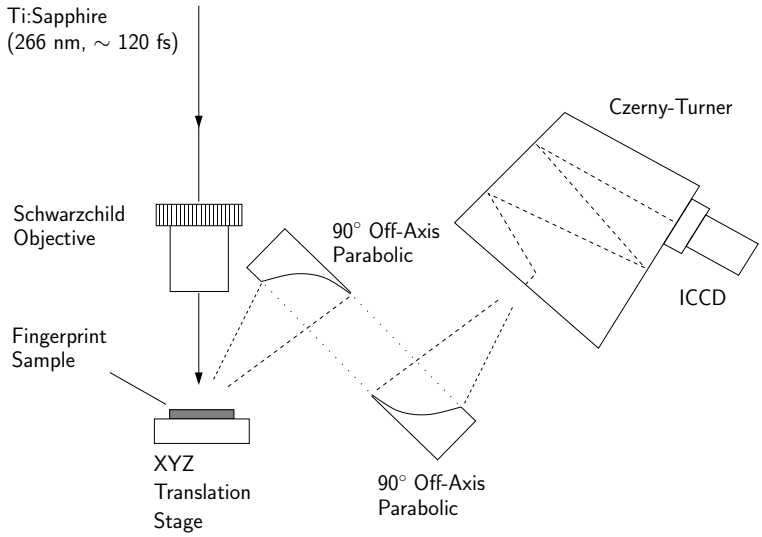

Figure 1. Schematic diagram of the setup used for μLIBS measurement of fingerprints.

Resonant dual-pulse LIBS technique have been studied by a number of groups [20–25]. The technique was first demonstrated by Kwong et al. in 1979, who measured the concentration of chromium in metal alloys and organic substances at the ppm level [20]. Most work has been performed with solid samples [20–23]. Recently the technique has been applied to liquid samples by Koch et al. [25], who measured the concentration of indium in bulk water samples. However, the high energies used to date, limit the portability of this technique. In this paper, the μLIBS technique is extended with a resonant dual-pulse method to enhance the LODs achievable with conventional μLIBS.

2 Experimental Setup

2.1 Fingerprint Detection

The experimental setup used to detect and map fingerprints is shown in Fig. 1. The pulses from a Ti:Sapphire (Spectra-Physics Hurricane) laser which produces $\sim$ 130 fs (FWHM) at 800 nm are frequency tripled to 266 nm, producing maximum pulse energies of $\sim$ 15 μJ on target. The pulse width of the tripled beam is estimated at $\sim$ 130 fs (FWHM) on target.

The beam was focused onto the target using a 15X Schwarzchild objective. The LIBS plasma emission was imaged 1:1 onto the spectrometer's entrance slit with a pair of 90° aluminum off-axis parabolic mirrors. A grating with 600 lines mm^{-1} and a blaze angle of 400 nm was used in the spectrometer giving a reciprocal linear dispersion of 0.168 nm channel^{-1} or 6.5 pm μm^{-1}. The entrance slit of the spectrometer was 100 μm for all experiments.

Spectra were recorded using an ICCD (Andor iStar DH720-25 mm). Due to the low pulse energies used in μLIBS, short delay times are necessary to achieve an optimum signal to noise ratio (SNR) [26, 27]. The delay time was calibrated using scattered laser light to measure the arrival time of the laser pulse at the target. A gate delay of 5 ns and gate width of 1 μs was used.

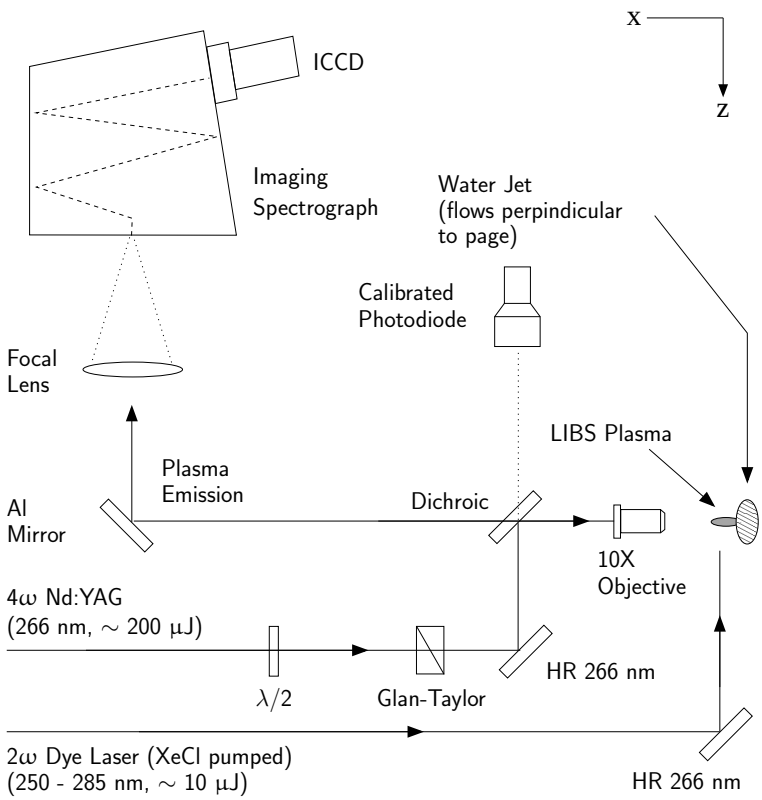

Figure 2. Schematic diagram of the LA-LIF setup. A frequency quadrupled Nd:YAG laser (266 nm, $\sim$ 10ns FWHM) with a pulse energy of $\sim$ 200 μJ, ablates the waterjet target. Pulse energy is controlled using a combination of a half-wave plate and Glan-Taylor prism. The energy of the ablation pulse is monitored using the calibrated photodiode. LIBS emission is observed along the laser axis.

The fingerprint preparation procedure described in [13] was used here.

2.2 Resonant Dual-Pulse μLIBS

The experimental setup used for the LA-LIF experiments is as shown in Fig.2. The ablation pulse used was typically 170 μJ, 10 ns pulse at 266 nm. The pulse was focused with a $10\times$ objective to form an approximately $\sim$ 10 μm diameter spot on the water jet. Different samples were prepared with different concentrations by weight of lead as analyte. The resonant excitation pulse was from a frequency-doubled XeCl-pumped dye laser with an energy of the order of 10 μJ and its pulse width was 9 ns. The spatial beam profile of the 2nd pulse at the location of re-excitation was 200 μm along the x and z directions. The timing of the resonant pulse was controlled by a delay generator (Stanford DG535), and the spatial re-excitation position of the resonant pulse was adjusted by the final tuning mirror. The wavelength was tuned to resonantly excite the 283.306 nm transition of Pb, which populated the Pb atoms from the ground state to the $7S_{1/2}$ state in accordance with the energy level diagram shown in Fig. 3. The probe wavelength was the 405.895 nm transition of the Pb atoms.

The plasma created was imaged in the x-y plane and projected onto the entrance slit of a 1/4 m, f/3.9 imaging spectrometer (Oriel MS260i) equipped with an intensified CCD (ICCD).

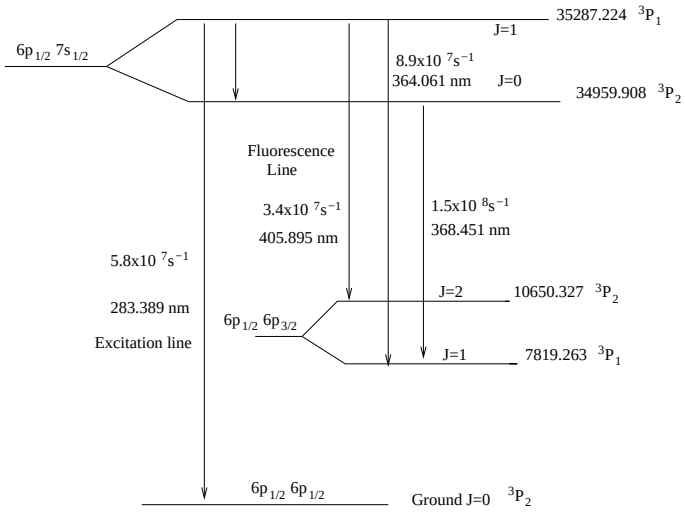

Figure 3. Simplified energy level diagrams for Pb. The laser excited transitions and the fluorescence transitions are indicated. The energies of the levels are indicated in wavenumbers [28].

A grating with 2400 lines mm^{-1} was employed. Some of the important factors that affect the Signal to Noise Ratio (SNR) in the LA-LIF experiment are the temporal separation between the two pulses (ΔT) and the re-excitation location in the plume and also the integration time of the signal. The LOD is defined as the point at which the signal obtained is 3σ above the average noise scaled to a bandwidth equal to that used to measure the emission line area. The expanding plasma was probed at different spatial positions and at different probe delay times in order to determine the conditions leading to the best SNR.

3 Results and Discussion

3.1 μLIBS Fingerprint Mapping

The scaling of Na emission from latent fingerprints on Si wafers was studied for laser pulses at 266 nm and energies below 15 μJ. An average of 100 single shots taken along a 5 mm line through the fingerprint were taken to quantify the average response of the latent fingerprints. Note that this averages the response over all positions in the fingerprint. The data presented in Fig. 4 is collected from three different fingerprints, all prepared in the same manner. It can be seen that there are some variations between the fingerprint samples but the data does show a consistent trend.

Using $\sqrt{N_{shots}}$ scaling and the data presented in Fig. 4, it is expected that the limit of single shot detection of Na will occur at $\sim$ 3.5 μJ. The current data was taken with a 100 μm slit. In the case of fingerprints on Si substrates, a much wider spectrometer slit can be used since the spectral signatures are well understood. Using a 500 μm slit width, a 2D map of a region of a thumbprint was acquired using a grid spacing of 50 μm. The analysis method was as presented previously in [13]. The resulting images are presented in Fig. 5. The fingerprint is clearly visible in the 5 μJ 2D map. The substrate shielding phenomena observed at higher energies is still observed here giving a negative print based on the detection of the second order 288.2

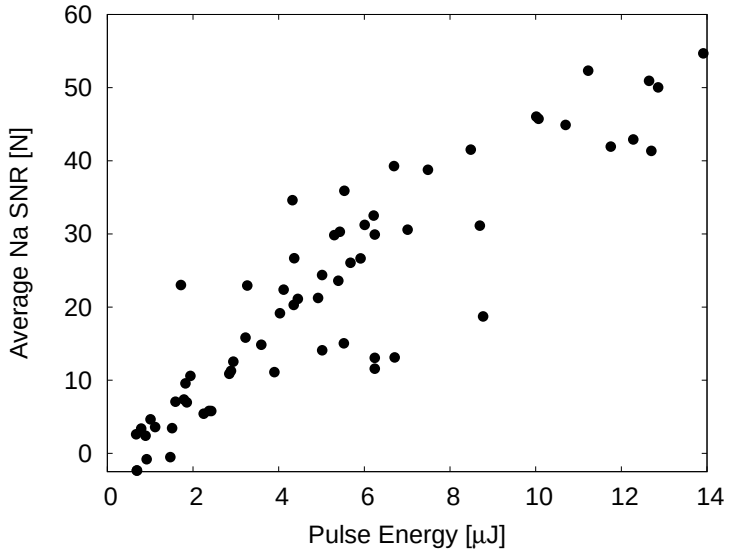

Figure 4. Fingerprint (Na) emission scaling for 266 nm, 130 fs pulses. The limit for reliable single shot detection of Na fingerprints is of the order of 3.5 μJ.

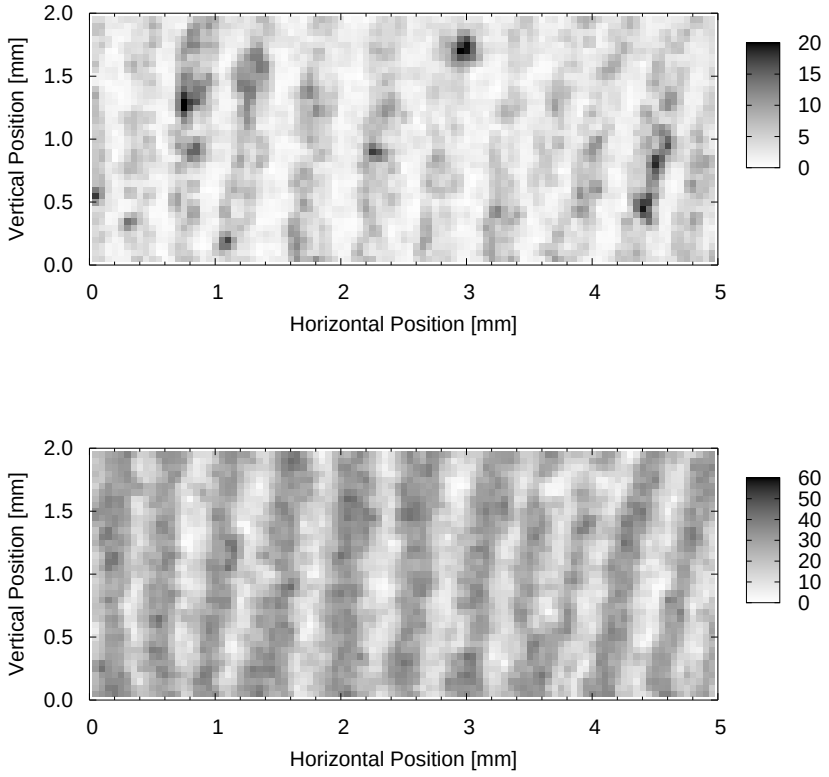

Figure 5. SNR of Na (top) and Si (bottom) for a portion of a latent fingerprint. The fingerprint ridges are clearly visible in both images.

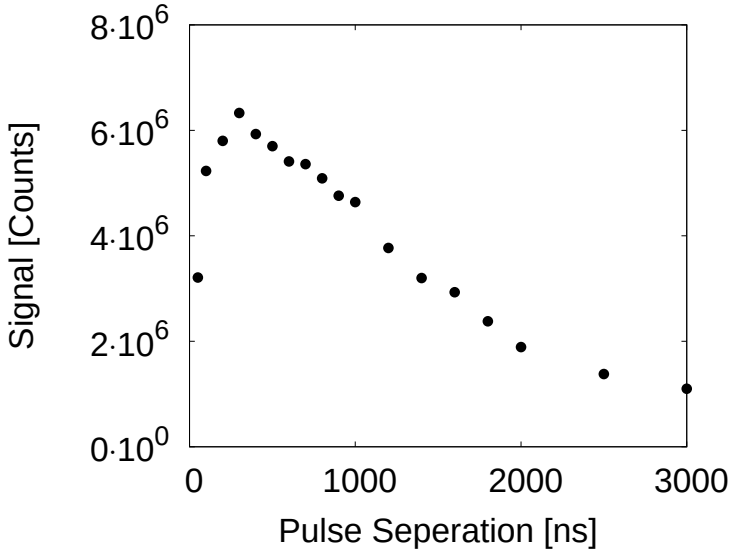

Figure 6. The SNR of the Pb emission spectra at different inter-pulse temporal separations is shown using the resonant dual-pulse technique.The ablation pulse energy used is 170 μJ. The resonant pulse energy is 8 μJ and the gate width for each spectra is 100 ns. At very small pulse separations the continuum masks the Pb emission signal whereas at the optimum pulse separation the continuum has decreased significantly.

nm Si line. At these pulse energies, it would be possible to discriminate fingerprint from the background Si substrate either by using the direct elemental signature of the print, or by the supression of the Si signature. This result demonstrates that the use of microchip or fiber lasers with a few μJ pulse energies would be suitable for a portable μLIBS fingerprint scanning system for simple smooth substrates such as Si wafers.

3.2 Resonant Dual-Pulse μLIBS of Pb

3.2.1 System Timing Optimization

The timing between the two laser pulses and the detector timing is very important to control in a μLIBS experiment. The probe time, or the pulse separation (ΔT), is critical to the signal enhancement. If the 2nd pulse re-excites the plume too early, the strong plasma continuum and competing line emission masks the enhancement of the signal due to the second excitation pulse. If the plume is re-excited too late, the plume will have expanded too much and only a small fraction of the species of interest can be excited. The ΔT was varied from 50 ns to 2300 ns and also the spatial postion for the maximum SNR was measured for each ΔT. Fig. 6.The best signal was obtained at a ΔT of $\sim$ 300 ns. A longer detector integration time is generally preferred because it leads to more signal integration. However, as the resonance enhanced Pb signal is short-lived, a longer integration time will only accumulate more intensifier noise spikes, which result in a higher noise level. To find the ideal integration window for our system, the ΔT and gate delay were fixed at 300 ns, the gate was turned on at a time when the re-excitation happens. The best SNR was obtained for a gate width of 10-20 ns which is consistent with the 10 ns excitation time and 10 ns lifetime of the Pb upper state.

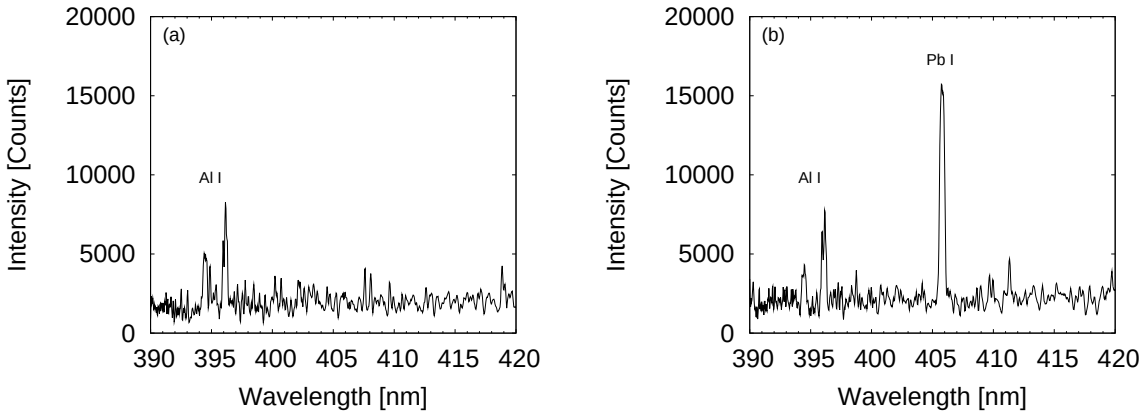

Figure 7. (a) The emission intensity for the single pulse μLIBS is shown for a sample containing 10 ppm of Pb and 150 ppm of Al as analyte. In the single pulse case we cannot detect Pb at such low concentrations. (b) The emission intensity of the same sample containing Pb and Al is shown. Here the plume was re-excited at the temporally and spatially optimum positions to selectively enhance the Pb atoms. The Al emission is the same as in the single pulse case but the emission of the Pb atoms is enhanced.

3.2.2 Scaling of Laser Pulse Energies

To find the optimum pulse energies both for ablation and re-excitation a parametric study of the effect of the two pulse energies was made. It was found that above an ablation energy of 170 μJ the emission signal does not increase significantly. The resonant pulse energy was also varied and it was found that pulses of the order of 10 μJ were sufficient to give full excitation of the plasma plume for 125 μJ ablation pulses.

3.2.3 Emission Line Spectrum and LOD

The selectivity of the emission enhancement is shown in Fig. 7 for a sample containing 10 ppm of Pb and 150 ppm of Al by weight in water. A probe delay time of 300 ns was chosen to enhance only the Pb emission where the emission of the residual Al lines was still visible.

Fig. 8 shows the LA-LIF spectrum of a sample containing 100 ppb of Pb by weight. A 10000 shot average yeilds a SNR of 12 which corresponds to a 1000-shot LOD of 73 ppb for Pb in our system.

4 Extension to Lab on a Chip Applications

The single and dual-pulse μLIBS techniques can be applied not only to waterjets but also microfluidic systems where the small laser energies would be compatible with the excitation of 10 μm scale size extruded droplets. Such applications include Lab on a Chip (LOAC) or micro-Total Analytic Systems (μTAS) for the analysis of very small fluid samples. A conceptual layout of such a device is shown in Fig. 9. Such systems could prove beneficial for point of care medical diagnostics of fluid composition as one specific application area.

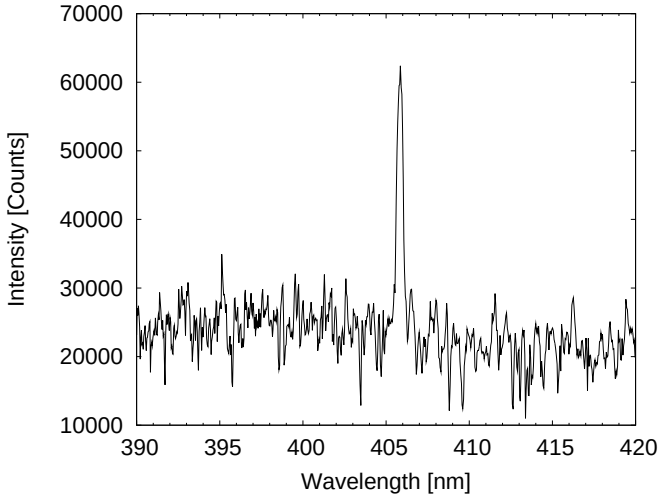

Figure 8. LA-LIF spectrum for a sample containing 100 ppb of Pb. The spectrum is an accumulation of 1000 shots. The gate width is set at 20 ns and the inter-pulse separation is 300 ns.

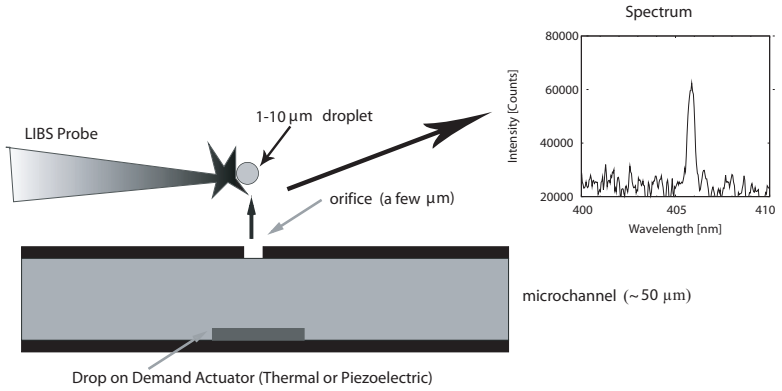

Figure 9. A droplet extrusion system using either a thermal or a piezoelectric technique to eject sample droplets for analysis of chemical composition.

5 Summary and Conclusions

We have demonstrated that by the resonant dual-pulse technique the sensitivity of the LIBS can be increased with orders in magnitude reduction in the ablation pulse energy, which makes the realization of a field portable spectrometer more realistic. Even though we are in the 100 ppb range for Pb significant improvements can be made. Possible approaches are to increase the resonant pulse energy, improve the collection optics and integrate more shots using higher repetition rate lasers. In addition, a more sophisticated analysis of the signal such as noise spike rejection and an emission line fitting approach may be employed.

A 2D map of a fingerprint on a Si wafer has been successfully acquired using 5 μJ pulses, demonstrating that fiber or microchip lasers with kHz repetition rates could be used as the excitation source for a portable μLIBS fingerprint scanner.

These μLIBS techniques can also be applied to microfluidic Lab on a Chip applications for the measurement of elemental content of micro specimens of fluids. Considerable work is

still required in order to determine the optimum configuration and LODs obtainable for such systems.

Acknowledgments

The authors gratefully acknowledge financial support for this research from both MPB Technologies Inc. and the Natural Sciences and Engineering Research Council of Canada.

References

[1] D.A. Cremers and L.J. Radziemski. *Handbook of Laser-Induced Breakdown Spectroscopy*. John Wiley & Sons, Ltd., 2006.
[2] A.Z. Miziolek, V. Palleschi and I. Schechter, editor. *Laser-Induced Breakdown Spectroscopy (LIBS): Fundamentals and Appl ications*. Cambridge University Press, 2006.
[3] J.R. Wachter, D.A. Cremers. *Applied Spectroscopy*, Vol. 41:1042 – 1054, 1987.
[4] C.M. Davies, H.H. Telle, A.W. Williams. *Fresenius Journal of Analytical Chemistry*, 355:895 – 899, 1996.
[5] E. Stoffels, P. van de Weijer, J. van der Mullen. *Spectrochimica Acta B*, Vol. 46:1459 – 1470, 1991.
[6] P. Fichet, P. Mauchien, C. Moulin. *Applied Spectroscopy*, Vol. 53:1111 – 1117, 1999.
[7] A.I. Whitehouse, J. Young, I.M. Botheroyd, S. Lawson, C.P. Evans and J. Wright. *Spectrochim. Acta, Part B*, Vol. 56:821 – 830, 2001.
[8] G.T. Razdobarin, G. Federici, V.M. Kozhevin, E.E. Mukhin, V.V. Semi, S.Y. Tolstyakov. *Fusion Science and Technology*, 41:32 – 43, 2002.
[9] V.I. Babushok, F.C. DeLucia Jr., P.J. Dagdigian, M.J. Nusca and A.W. Miziolek. *Applied Optics*, Vol. 42:5947 – 5962, 2003.
[10] G.W. Rieger, M. Taschuk, Y.Y. Tsui and R. Fedosejevs. *Applied Spectroscopy*, Vol. 56:689 – 698, 2002.
[11] I. Cravetchi, M. Taschuk, G.W. Rieger, Y.Y. Tsui and R. Fedosejevs. *Applied Optics*, Vol. 42:6138 – 6147, 2003.
[12] I. Cravetchi, M. Taschuk, Y.Y. Tsui and R. Fedosejevs. *Spectrochimica Acta B*, 59:1439 – 1450, 2004.
[13] M.T. Taschuk, Y.Y. Tsui and R. Fedosejevs. *Applied Spectroscopy*, 60:1322 – 1327, 2006.
[14] B.E. Dalrymple, J.M. Duff and E.R. Menzel. *Journal of Forensic Sciences*, 22:106 – 115, 1976.
[15] Li Wenchong, Ma Chunhua, Jiang Hong, Wu Chengbai, Lu Zhiming, Wang Bangrui and Lu Bingqun. *Journal of Forensic Sciences*, 37:1076 – 1083, 1992.
[16] S.K. Bramble, K.E. Creer, W. Gui Qiang and B. Sheard. *Forensic Science International*, 59:3 – 14, 1993.
[17] U.S. Dinish, L.K. Seah, V.M. Murukeshan, L.S. Ong. *Optics Communications*, Vol. 223:55 – 60, 2003.
[18] U.S. Dinish, Z.X. Chao, L.K. Seah, A. Singh and V.M. Murukeshan. *Applied Optics*, Vol. 44:297 – 304, 2005.
[19] C. Lopez-Moreno, S. Palanco, J.J. Laserna, F. DeLucia, A.W. Miziolek, J. Rose, R.A. Waters and A.I. Whitehouse. *J. Anal. At. Spectrom.*, Vol. 21:55 – 60, 2006.
[20] H.S. Kwong, R.M. Measures. *Analytical Chemistry*, Vol. 51:428 – 432, 1979.
[21] V. E. Bondybey, and J. H. English. *Journal of Chemical Physics*, Vol. 74:6978 –, 1981.
[22] W. Sdorra, A. Quentmier, K. Niemax. *Mikrochimica Acta*, Vol. 98:201 – 218, 1989.
[23] I. B. Gornushkin, J. E. Kim, B. W. Smith, S. A. Baker, J. D. Winefordner. *Applied Spectroscopy*, Vol. 51:1055 – 1059, 1997.
[24] R.E. Neuhauser, U. Panne, R. Niessner, G.A. Petrucci, P. Cavalli, and N. Omenetto. *Analytica Chimica Acta*, pages 37 – 48, 1997.
[25] S. Koch, W. Garen, W. Neu, R. Reuter. *Analytical and Bioanalytical Chemistry*, Vol. 385:312 – 315, 2006.
[26] H. Häkkänen and J.E.I. Korppi-Tommola. *Applied Spectroscopy*, Vol. 49:1721 – 1728, 1995.
[27] G.W. Rieger, M. Taschuk, Y.Y. Tsui and R. Fedosjevs. *Spectrochimica Acta B*, Vol. 58:497 – 510, 2003.
[28] D. R. Jenkins. *Proc. Roy. Soc. Lond. A.*, Vol. 313:551–564, 1969.